THE JOURNAL OF PHYSICAL CHEMISTRY B
A JOURNAL OF THE AMERICAN CHEMICAL SOCIETY

pubs.acs.org/JPCB

Article

Dynamic Duo: Vibrational Sum Frequency Scattering Investigation of pH-Switchable Carboxylic Acid/Carboxylate Surfactants on Nanodroplet Surfaces

Marc J. Foster, Andrew P. Carpenter, and Geraldine L. Richmond*

Cite This: *J. Phys. Chem. B* 2021, 125, 9629–9640

Read Online

ACCESS | Metrics & More | Article Recommendations | Supporting Information

ABSTRACT: Surfactants containing pH-switchable, carboxylic acid moieties are utilized in a variety of environmental, industrial, and biological applications that require controlled stability of hydrophobic droplets in water. For nanoemulsions, kinetically stable oil droplets in water, surface adsorption of the anionic form of the carboxylic acid surfactant stabilizes the droplet, whereas a dominant surface presence of the neutral form leads to destabilization. Through the use of dynamic light scattering, ζ-potential, and vibrational sum frequency scattering spectroscopy (VSFSS), we investigate this mechanism and the relative surface population of the neutral and charged species as pH is adjusted. We find that the relative population of the two surfactant species at the droplet surface is distinctly different than their bulk equilibrium concentrations. The ζ-potential measurements show that the surface concentration of the charged surfactant stays nearly constant throughout the stabilizing pH range. In contrast, VSFSS shows that the neutral carboxylic acid form increasingly adsorbs to the surface with increased acidity. The spectral features of the headgroup vibrational modes confirm this behavior and go further to reveal additional molecular details of their adsorption. A significant hydrogen-bonding interaction occurs between the headgroups that, along with hydrophobic chain−chain interactions, assists in drawing more carboxylic acid surfactant to the interface. The charged surfactant provides the stabilizing force for these droplets, while the neutral surfactant introduces complexity to the interfacial structure as the pH is lowered. The results are significantly different than what has been found for the planar oil/water studies where stabilization of the interface is not a factor.

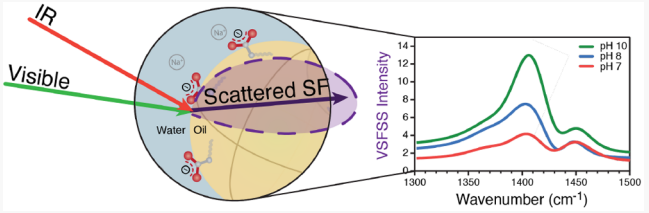

INTRODUCTION

Carboxylic acid containing surfactants, or fatty acids, are ubiquitous in biological, industrial, and environmental systems.[1−4] They are building blocks for complex polar lipids such as triglycerides capable of storing energy for microbes,[5] are found in many cleaning substances as a nontoxic soap,[6] and are often used in remediation efforts due to the switchable nature of the headgroup.[7] The reason these types of surfactants are found in so many processes is because of the diverse and complex chemical interactions of the headgroup.[4,6,8−16] They have been shown to readily bind to metals,[8] can easily be formed through hydrolysis reactions of more complex starting material,[10] and can have varied functionality and adsorptive properties by simple protonation and deprotonation of the headgroup.[9,11] This last point has made carboxylic acids of particular interest in oil spill remediation efforts as the protonated headgroup is much less hydrophilic than its deprotonated counterpart.[12] Furthermore, the pH switchability of the surfactant can be used to stabilize oil droplets when the headgroup is charged and destabilize the oil droplets when the headgroup is neutral.[13,14] This has allowed for enhanced ability in removing oil from contaminated sands, which is notoriously hard to remediate.[15] Often in these remediation efforts a simplified picture of interfacial activity is presented based on solubility. It is concluded that the protonated headgroup (less soluble) switches off interfacial activity while the deprotonated headgroup (more soluble) switches on interfacial activity to the emulsion surface.[16] However, this may not be entirely accurate as the protonated species are still amphiphilic molecules that would adsorb to an interface, and recent studies at the planar air/water interface suggest a more complex picture. These studies find a synergistic surface interaction between the protonated and deprotonated forms that leads to an overall increase in the adsorption of both species to the surface.[17]

Numerous studies of carboxylic acid containing surfactants at planar liquid and solid interfaces have provided useful information about how these surfactants adsorb and assemble at liquid surfaces.[8,18−25] Such planar studies are a good starting point for understanding their surfactant adsorption in colloidal systems. However, for the special case of surfactant-stabilized

Received: June 22, 2021
Revised: July 27, 2021
Published: August 17, 2021

nanoemulsions, on the size scale of 200−500 nm in diameter, direct comparison might be less applicable since they are formed in a kinetically stable state as opposed to the more favorable thermodynamic state of the planar oil/water interface.[26] In these cases, surfactants act as essential components to form and stabilize the nanoemulsion oil/water interface. The presence of these molecules helps prevent coalescence, Ostwald ripening, flocculation, or other methods of destabilization in which the oil droplets change in size and become polydisperse, eventually phase separating into the respective oil and water layers.[27] In the case of planar systems the interface does not require stabilization, and amphiphilic molecules simply adsorb to the surface. This difference in interfacial energetics as well as the different roles of the surfactant could pose changes to the molecular structure between the two surfaces. Nanoemulsions have been shown to be good model systems to understand the molecular details of curved interfaces, and they also have a growing number of applications in technology and medicine.[2,28−36] Obtaining molecular level information about suspended droplets of this size has traditionally been quite difficult. However, more recently vibrational sum frequency scattering spectroscopy (VSFSS) has emerged as a valuable tool for obtaining such molecular level information about nanoemulsion stability and interfacial structure as this technique can probe the molecular details of colloidal systems.[28,30,32−39] These molecular details can then be used to more accurately understand the factors contributing to the stabilization of these droplets.

This study takes advantage of the pH-dependent charge switchability of alkyl carboxylic acid containing surfactants to understand how surfactant adsorption and its charge play a role in the stabilization of nanoemulsions. Using a combination of VSFSS, dynamic light scattering, and ζ-potential measurements, we provided new insights about the molecular structure of carboxylic acid surfactant stabilized nanodroplet surfaces, as the bulk solution is varied from low to high pH. The results show that the droplets remain stable only when there is some amount of charged carboxylate surfactant present at the interface and destabilize when the mixture contains solely neutral carboxylic acid surfactant. In the pH region where the nanoemulsions are stable, measurements of charge suggest a stagnant interfacial structure. While stability and charge indicate a simple adsorption behavior to the surface, VSFSS reveals that the interfacial structure and adsorption interplay between the protonated and deprotonated surfactants are remarkably more dynamic with pH than was originally thought.

MATERIALS AND METHODS

Materials and Sample Preparation. All materials were purchased with the highest purity and used as delivered with no further purification. Sodium octanoate (≥98%), decanoate (≥98%), dodecanoate (≥98%), hexadecane (≥99%), and dioctyl sodium sulfosuccinate (AOT, ≥97%) were purchased from Sigma-Aldrich. Deuterated decanoate (d-decanoate, 98% D), deuterated hexadecane (d-hexadecane, 98.6% D), sodium deuteroxide (NaOD, 99.5% D), and deuterium chloride (DCl, 99.9% D) were purchased from CDN Isotopes. Deuterium oxide (D_2O, 99.9% D) was purchased from Cambridge Isotope Laboratories. All glassware was thoroughly cleaned in a sulfuric acid (98%, Sigma-Aldrich) bath containing AlNOCHROMIX oxidizer from Godax Laboratories Inc. The acid-washed glassware was rinsed for 3 min under 18.2 MΩ·cm water and dried in an oven.

Nanoemulsions were prepared through ultrasonication. An initial emulsion solution containing a small amount of surfactant (sodium octanoate, decanoate, dodecanoate, or AOT) was sonicated with twice the amount of hexadecane oil to be 2% v/v oil in water. The emulsion samples used for spectroscopy and ζ-potential were created by taking equal volumes of the 2% emulsion solution and an aqueous solution containing the necessary surfactant concentration and DCl (HCl) or NaOD (NaOH) to reach the desired concentration and pD (pH). The end results were emulsion samples that were 1% v/v hexadecane in an aqueous solution of surfactant at the desired pH. MilliporeSigma MColorpHast pH strips were used to determine the pH of the nanoemulsion samples. In the paper pH is used for ease instead of switching between pH and pD, although it is noted that detection of pH values can differ than pD values by 0.43.[40] The concentrations used in these experiments were purposely kept below the CMC of the surfactants, reported as 300 mM (octanoate), 100 mM (decanoate), and 28 mM (dodecanoate).[41,42] The surfactant concentration used for the ζ-potential was lower than for the spectroscopic studies as the ζ-potential requires an electrochemical potential to be applied to the solution. High ionic strength solutions undergo reactions at the electrodes, producing bubbles that interfere with the measurement, resulting in inconsistent and noisy data. Low ionic strength solutions do not see these interferences.

Dynamic Light Scattering and ζ-Potential. Dynamic light scattering (DLS) and ζ-potential measurements were used to characterize the size and surface charge, respectively, of the nanoemulsions. DLS and ζ-potential experiments were conducted by using a Malvern Zetasizer Nano ZS. Size measurements for all nanoemulsions were made and used only if the distribution was monomodal. The average size prepared was ∼300 nm in diameter. They were used only if the polydispersity index (PDI) was at or below 0.250. Included in the Supporting Information is information about stability of the emulsions as well as size distribution plots, *z*-average diameters, and the given polydispersity index for a representative emulsion experiment. The stability of the nanoemulsions is determined to be the invariance and the monodispersity of the particle size distribution of the sample over time. Additionally, stability was gauged visually as the nanoemulsions in the size range studied (∼300 nm in diameter) produce an opaque liquid. The persistence of this opaque liquid indicates stable nanoemulsions and is confirmed by taking size distribution measurements over time. Unstable nanoemulsions will become clear over a short period of time, and their size distributions will result in multiple peaks. For the DLS experiments, three measurements were made and averaged for each sample. For the ζ-potential experiments, 10 measurements were made and averaged for each sample.

Vibrational Sum Frequency Scattering Spectroscopy. Vibrational sum frequency is a second-order, nonlinear, spectroscopic technique that uses the spatial and temporal overlap of a fixed visible and a tunable IR laser beam to probe molecular structure of an interface.[44] A sum frequency response is forbidden in centrosymmetric environments, such as bulk solutions. This technique is therefore widely used to study interfacial molecular structure and chemistry as interfaces inherently break centrosymmetry. When the IR beam is chosen to be resonant with a vibrational mode that is

https://doi.org/10.1021/acs.jpcb.1c05508
J. Phys. Chem. B 2021, 125, 9629−9640

both Raman- and IR-active, and ordered at the interface, the sum frequency response is enhanced, effectively resulting in a vibrational spectrum of adsorbed molecules. Most commonly, sum frequency is used on planar surfaces (air/water, oil/water, or solid/water). The theory for planar sum frequency has been thoroughly developed, and shows that sum frequency intensity is sensitive to both population and orientation of the probed dipole moments.[45−47] Roke et al. developed the theory and implementation of sum frequency scattering[30,31,48] (Figure 1), which follows much of the same selection rules as planar sum frequency but can probe molecular structure and chemistry of suspended particles in solution.

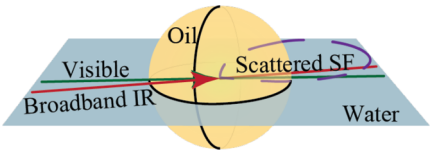

Figure 1. VSFSS experimental geometry, with the visible pulse depicted in green, IR pulse in red, and the scattered sum frequency (SF) response in purple.

The laser system used has been detailed previously[36] and consists of a Libra series (Coherent) Ti:sapphire amplifier which outputs a fundamental 800 nm beam at 1 kHz repetition rate with an ∼100 fs pulse width. This 800 nm beam is sent to an optical parametric amplifier (OPA) where a beam splitter sends part of the beam directly out of the OPA to the experimental stage. This is used as the visible pulse to achieve sum frequency at the sample stage. The other part of the beam is sent through the OPA to generate the broadband IR pulse through difference frequency generation. The visible pulse is sent through an etalon which stretches the pulse asymmetrically in time so that at the sample stage it has a picosecond pulse width. This gives a spatial resolution in our spectra of 8 cm^{-1}. At the sample stage, the sum frequency response is collimated through a plano-convex lens and then focused by a focusing lens. The sum frequency light is collected at a 60° scattering angle relative to the phase matching direction, measured by the sum frequency generated out of a sum frequency crystal. The collected sum frequency light is sent through a spectrometer and spectrally dispersed onto a CCD camera.

The polarizations of the sum frequency, visible, and IR used in these studies were ssp and ppp. The letters in the polarization abbreviation correspond to the polarization of the sum frequency, visible, and IR beams, respectively. The energy of the visible pulse was held at 25 μJ. The IR pulse energy was ∼5, ∼4, and ∼3 μJ for the CH, C═O, and COO^- stretching regions, respectively. The nanoemulsion samples were held in a 200 μm path length cuvette that consisted of a CaF_2 front window and a SiO_2 back window, with a thickness of 1.3 mm for each window. Each spectrum was normalized to a $KNbO_3$ nanoparticle nonresonant response, which captures the power profile of the broadband IR beam. Significant water vapor absorption occurs in the IR region for the COO^- stretch (1300−1500 cm^{-1}) and C═O stretch (1600−1800 cm^{-1}). In these cases, the experimental stage was purged with dry air to a humidity of 4%. Every spectrum is the average of at least three runs obtained from different days, with each run consisting of two 20 min scans background subtracted with two 20 min background scans.

Spectral Fitting. The sum frequency intensity is proportional to the intensity of the two incoming beams as well as the square of the effective second-order nonlinear susceptibility ($\Gamma^{(2)}$).[31,47] The effective nonlinear susceptibility encompasses the shape of the particle, and the second-order nonlinear susceptibility ($\chi^{(2)}$). The $\chi^{(2)}$ component describes the nonlinear response at the interface which can be broken up into a nonresonant and resonant contribution. The resonant contribution contains information about the orientation and population of the resonant vibrational dipole moment probed. The spectra were fit by using a procedure that follows previous Richmond group analysis,[49] based on a procedure described by Bain et al.[50] This describes the origin of the $\chi^{(2)}$ response, given as a convolution of a Lorentzian and Gaussian distribution:

$$\chi_\nu^{(2)} \propto A_{NR} e^{i\psi} + \sum_\nu \int \frac{A_\nu e^{i\psi_\nu} e^{-[(\omega_L-\omega_\nu)/\Gamma_\nu^2]^2}}{\omega_L - \omega_{IR} + i\Gamma_L} d\omega_L \quad (1)$$

Equation 1 takes into account the homogeneous broadening (Γ_L) due to the natural decay of the vibrational mode probed and the inhomogeneous broadening (Γ_ν) arising from the molecular environment of the mode. Each peak in the spectra was fit by using five parameters: amplitude (A_ν), phase (ψ_ν), Lorentzian line width (Γ_L), peak position frequency (ω_ν), and Gaussian line width (Γ_ν). Additionally, each spectrum was fit to a nonzero nonresonant component with two parameters: nonresonant amplitude (A_{NR}) and phase (ψ). All fit parameters and associated errors can be found in the Supporting Information.

RESULTS AND DISCUSSION

In aqueous mixtures of carboxylate surfactant, the proportion of protonated (carboxylic acid) to deprotonated (carboxylate) in the bulk is affected by changing the pH of the solution. Figure 2 shows the bulk percent protonation for three

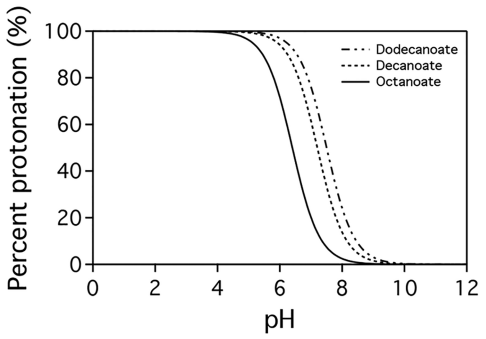

Figure 2. Computed percent protonation based on acid−base equilibrium expressions as a function of pH for sodium octanoate (solid line), decanoate (dashed line), and dodecanoate (dashed and dotted line).

surfactants sodium octanoate, decanoate, and dodecanoate as a function of pH (see the Supporting Information for a discussion on derivation).[15] The pK_as of aqueous carboxylate surfactants are reported in the range of ∼4−7.5.[51] At pH < 4, below the pK_a, the three systems are fully protonated in the bulk. At pH > 10 above the pK_a, the systems are fully deprotonated in the bulk. Between these two pH extremes, the bulk mixture contains a combination of carboxylic acid and carboxylate surfactants. Interfacial pK_as have been shown to

https://doi.org/10.1021/acs.jpcb.1c05508
J. Phys. Chem. B 2021, 125, 9629−9640

increase at an interface.[19,52] Additionally, there has been evidence for pK_a changes on nanoparticles due to curvature differences in nanoparticle sizes.[53] Thus, the bulk composition of the surfactant mixture may not necessarily reflect the interfacial composition but still can be used to give a qualitative picture of the surfactant available to adsorb to the interface. The adsorption behaviors of these mixtures with pH have been investigated at the oil/water and air/water planar interfaces by using a variety of techniques.[17,18,22] Planar studies show that the charged carboxylate surfactant on its own preferentially adsorbs to the oil/water interface, adopting a significant degree of net orientation, while the neutral carboxylic acid surfactant on its own is present in small amounts but has only a small degree of net orientation.[18] With a mixture of carboxylic acid and carboxylate surfactants there is thought to be the formation of acid−anion complexes at the planar air/water interface and in the bulk, which was not observed at the planar oil/water interface.[54,55]

To begin characterization of carboxylic acid-stabilized nanoemulsions, ζ-potential measurements were conducted to examine their surface potential as a function of pH. Figure 3

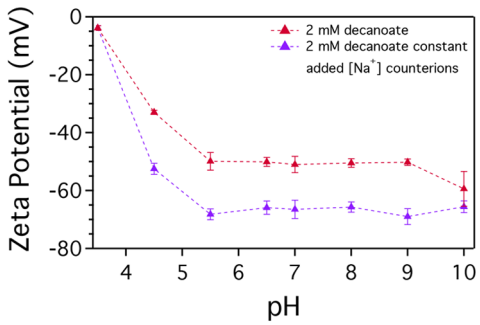

Figure 3. ζ-potential for 2 mM decanoate (red triangles) stabilized nanoemulsions, and 2 mM decanoate stabilized nanoemulsions at constant added counterion (Na^+) concentration (purple triangles) all as a function of pH. Constant counterion concentration (purple triangles) was maintained by added necessary amounts of NaCl to reach a counterion concentration of 34.9 mM.

shows the ζ-potential values for nanoemulsions stabilized with the surfactant sodium decanoate as a function of pH and decanoate at a constant concentration of added Na^+ counterions as a function of pH (bottom trace). The constant concentration of counterions was fixed to 34.9 mM by adjusting accordingly with the necessary amount of NaCl given the amount of added NaOH needed to reach each pH condition. As shown in Figure 3, the ζ-potential reaches close to zero at a pH of 3.5 where the bulk mixture is fully protonated. Below pH 3.5 the nanoemulsions are not stable, consistent with the dominance of protonated surfactants in the bulk solution. At pH 3.5 the nanoemulsions quickly destabilize, indicated by size measurements exceeding 1000 nm in diameter within an hour, followed by the solution visually clearing to form separated oil and water layers (Figure S3). In the pH region of 5.5−10, these nanoemulsions are found to remain stable for months (Figure S2) and have a significant amount of interfacial charge, with a ζ-potential in the range of −40 to −60 mV. We attribute the main source of stability of these nanoemulsions to the charged, deprotonated surfactant at the nanodroplet surface. The presence of this interfacial charge limits coalescence through charge−charge repulsion between droplets.

As the pH increases from 3.5 to 5.5, the ζ-potential becomes more negative, indicating that the population of carboxylate surfactant to the interface is increasing. If we assumed a similar trend in deprotonation at the surface as seen in the bulk (Figure 2), one might expect that as deprotonation increases with increasing pH in the bulk, the ζ-potential would also progressively decrease with increased carboxylate adsorption. Instead, as the pH increases from 5.5 to 9 the ζ-potential remains constant. This pH region is also where the bulk surfactant shows the most rapidly changing percent protonation/deprotonation (Figure 2). Because the carboxylate form of the surfactant is the charge carrier in these systems, we conclude that this constancy in the ζ-potential value between pH 5.5 and pH 9, for all traces, reflects a constancy in the surface concentration of carboxylate surfactant.

Beyond pH 9 where the surfactant is fully deprotonated in the bulk, the ζ-potential for sodium decanoate without fixing the added counterion concentration shows a slight decrease (Figure 3, top trace). To test whether this effect is due to the results of percent protonation changes or due to the variation in counterion concentrations of the solution from the added base, analogous studies were performed for decanoate with the added counterion concentration held constant (Figure 3, bottom trace). Under these conditions, the ζ-potential remains constant albeit at a more negative value for all pHs tested above 5.5. We attribute the more negative ζ-potential value to increased carboxylate adsorption caused by the added counterions that reduce nearby repulsive headgroup interactions.[56] Hence, from the constancy in the ζ-potential for the fixed ionic strength, we conclude that the decrease in ζ-potential above pH 9 when the counterion concentration was not fixed (Figure 3, top traces) is due to increased counterions from the added base reducing the repulsive forces between neighboring surfactants. This reduction in repulsive forces allows more carboxylate species at the interface causing the decrease in ζ-potential and is not the effect of the bulk percent protonation changing with pH. From these results we conclude the carboxylate surfactant at the interface reaches a constant level through the pH range of 5.5−10 which contrasts with the bulk concentration of carboxylate that increases as the pH is increased (Figure 1). This would indicate the amount of carboxylate surfactant at the nanoemulsion surface relative to the bulk is small at all pHs above 5.5. An alternative possibility for the constancy in surface concentration of carboxylate species as the pH approaches 5.5 is that the increased carboxylic acid surfactant adsorption with lowered pH (as confirmed later in this paper) reduces the electrostatic repulsion between neighboring carboxylate surfactants. This could result in more carboxylate surfactant than might be expected at lower pH. This, however, is inconsistent with our constant counterion concentration ζ-potential studies, showing reduced electrostatic repulsion results in increased adsorption of carboxylate species. Surfactant limitation by charged repulsion on liquid and droplet surfaces is further supported by previous work.[18,22,29,32,33,56]

In planar air/water studies with bulk mixtures of carboxylic acid and carboxylate surfactants, it is often concluded that acid−anion pairs form at the interface.[17,22] In these studies, surface tension and planar sum-frequency indicate an increase in surface concentration of both the carboxylate and carboxylic acid species around the pK_a of the surfactant, making these

https://doi.org/10.1021/acs.jpcb.1c05508
J. Phys. Chem. B 2021, 125, 9629−9640

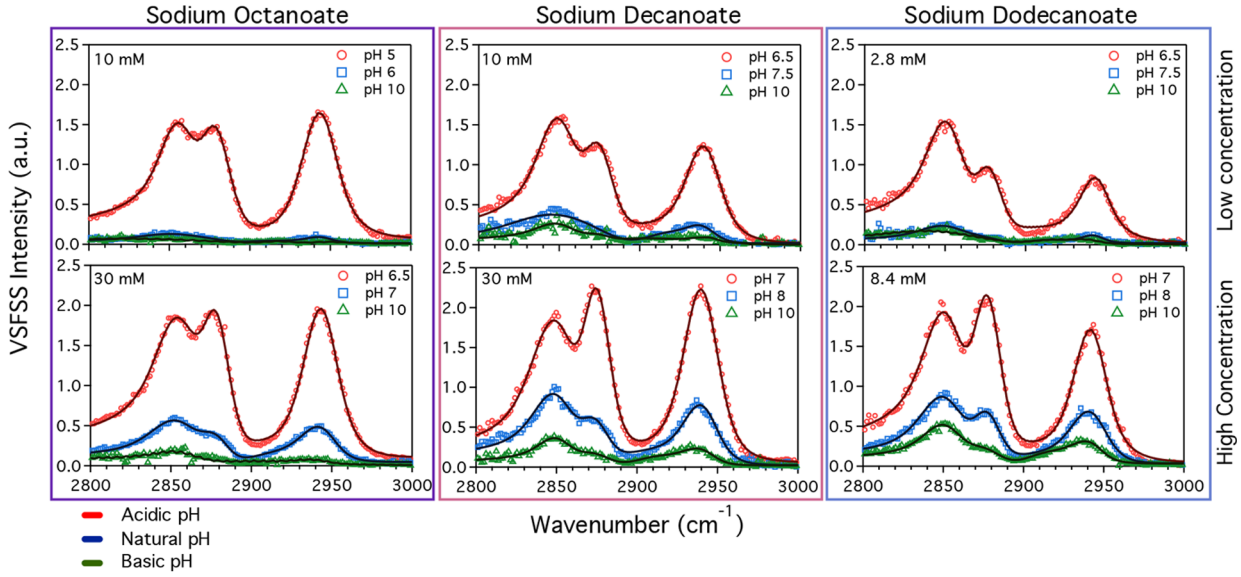

Figure 4. VSFSS spectra in ssp polarization of sodium octanoate (left panel), decanoate (middle panel), and dodecanoate (right panel) stabilized nanoemulsions with d-hexadecane, in D_2O, as a function of pH and concentration. Top row: low surfactant concentration spectra; bottom row: high surfactant concentration spectra. The red traces have DCl added, blue traces have no added DCl or NaOD, and green traces have NaOD added. Solid lines are fits to the spectra, with each surfactant system globally fit with each other.

complexes more surface active then each form on its own. For the nanodroplet surface the surface concentration of carboxylate species increases from pH 3.5 until pH 5.5. Then, there exists a limit to the surface concentration of carboxylate surfactant as pH increases, even as the carboxylate concentration in bulk continues to increase. Because ζ-potential does not report on carboxylic acid surfactant adsorption, the formation of acid−anion complexes at the emulsion surface is explored further by using VSFSS as described below.

VSFSS was used to probe the surface of the nanodroplets in three IR spectral regions to capture the vibrational response from the alkyl CH stretch modes (2800−3000 cm^{-1}), the carboxylate stretch modes (1300−1500 cm^{-1}, deprotonated headgroup), and the carbonyl stretch modes (1600−1800 cm^{-1}, protonated headgroup) of the adsorbed surfactants. Figure 4 shows CH VSFSS data in the ssp polarization combination for nanoemulsions stabilized with the three different surfactants as a function of pH, and concentration, in D_2O. The hexadecane oil was deuterated to shift these CH modes outside of the vibrational window probed. As shown in Figure 4, the CH modes from all three surfactants were examined as a function of pH with the lowest pH (red), midrange pH (blue), and highest pH (green) traces. The amount of DCl or NaOD added for each of the same-colored trace was constant, resulting in slightly different pHs for each system studied due to the differing pK_as of each surfactant. The red traces had DCl added with pH ranges for the systems between 5 and 7, the blue traces had no added DCl or NaOD with pH ranges between 6 and 8, and the green traces had NaOD added all resulting in pHs of 10. In all cases the spectra were globally fit to four peaks and a background response. The four peaks are assigned as such: ∼2855 cm^{-1}(methylene symmetric stretch), ∼2878 cm^{-1} (methyl symmetric stretch), ∼2930 cm^{-1} (methylene Fermi resonance), and ∼2940 cm^{-1}(methyl Fermi resonance).[8,18] At low wavenumbers there is a slight background elevation present in the spectra. It should be noted that there has been much discussion about the $\chi^{(3)}$ effect on sum frequency spectra of charged surfaces. This effect can present as a background response that is modulated by the sign and strength of an interfacial field. Although we do not explicitly identify this $\chi^{(3)}$ effect here, the elevated background seen in Figures 4 and 5, as will be shown,

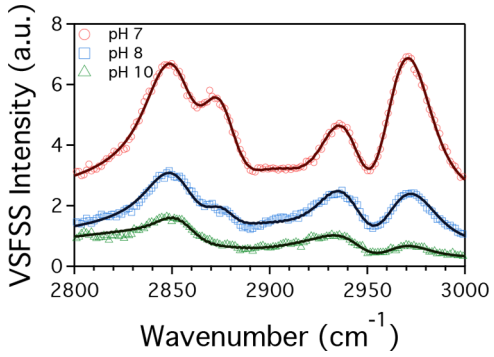

Figure 5. VSFSS spectra in ppp polarization for 30 mM sodium decanoate stabilized nanoemulsions in D_2O at pH 7 (red circles), 8 (blue squares), and 10 (green triangles). The spectra were globally fit, with solid lines representing the fits to each spectrum. The spectra are not offset from each other; rather, a significant background is presently seen often in sum frequency scattering experiments as a dispersive D_2O background.

could be due to this response.[43] A full discussion on the other possible contributions to this background and how this is accounted for in the fits is given in the Supporting Information.

Figure 4 shows a consistent trend as a function of pH for all spectra. The overall sum frequency response for the combined CH modes significantly increases as the solution goes from basic to acidic (green to red). At the basic pH the CH signal is dominated by just carboxylate surfactant, as there is almost no carboxylic acid surfactant present in the bulk mixture that could adsorb to the interface (Figure 2). From the above-described ζ-potential measurements, we know the carboxylate surfactant interfacial concentration remains constant from 5.5

https://doi.org/10.1021/acs.jpcb.1c05508
J. Phys. Chem. B 2021, 125, 9629−9640

to 10. However, the large increase in intensity as the pH is lowered for all peaks indicates increased overall interfacial population. We conclude that the growth in CH response with lowered pH is due to the adsorption of neutral carboxylic acid surfactant. Given that the nanodroplets are unstable when the bulk solution has only carboxylic acid surfactant below pH 3.5, it is interesting that we see such a large change in the adsorption behavior of the protonated carboxylic acid surfactant as the pH is lowered. The trend is consistent across all three surfactant tail lengths as well. The increase in hydrophobicity of the tails as the chains get longer does not significantly impact the surfactant adsorption behavior with pH. This means subtle differences in the hydrophobic interactions does not greatly affect the interfacial behavior.

Another key piece of information in understanding the adsorption behavior observed is detailing the conformational order of the alkyl tails with pH. This is done by measuring the amplitude ratio of the methylene symmetric stretch (d^+) to the methyl symmetric stretch (r^+). This ratio provides information about the relative degree of conformational order in the alkyl tails of the surfactant. An increasing number of gauche defects in the linear alkyl tail will result in a higher methylene peak and a lower methyl peak. Thus, a high d^+/r^+ ratio indicates conformational disorder, whereas a low d^+/r^+ ratio indicates conformational order of the alkyl tails.[44,57,58] Table 1 shows

Table 1. d^+/r^+ Ratios for Spectra in Figure 4[a]

10 mM octanoate		10 mM decanoate		2.8 mM dodecanoate	
pH	d^+/r^+	pH	d^+/r^+	pH	d^+/r^+
5	0.8 ± 0.1	6.5	1.0 ± 0.1	6.5	1.2 ± 0.1
6	1.9 ± 1.3	7.5	2.4 ± 0.7	7.5	1.5 ± 0.4
10	6.1 ± 7.5	10	2.1 ± 0.8	10	6.7 ± 6.1
30 mM octanoate		30 mM decanoate		8.4 mM dodecanoate	
pH	d^+/r^+	pH	d^+/r^+	pH	d^+/r^+
6.5	0.8 ± 0.1	7	0.8 ± 0.1	7	0.7 ± 0.1
7	1.4 ± 0.2	8	1.3 ± 0.1	8	1.1 ± 0.1
10	2.6 ± 1.5	10	1.1 ± 0.2	10	1.3 ± 0.1

[a]Ratios and error were calculated by using the amplitudes and error derived from the fits in the corresponding spectra. Concentration and pHs are listed for each system.

the d^+/r^+ ratio from the fits of the ssp CH data in Figure 4. As shown, the d^+/r^+ ratio decreases for all spectra series as the pH decreases. This indicates the alkyl tails are adopting more order as the pH is lowered. Higher ordered tails are typically associated with a more tightly packed interface, as the increased packing leads to increased hydrophobic interactions between neighboring alkyl chains. This is consistent with the view derived above, that the interfacial packing increases as more carboxylic acid adsorbs at the nanodroplet surface.

To further demonstrate that the surface concentration of the carboxylic acid surfactant increases as pH is lowered, Figure 5 shows VSFSS spectra for a pH series of nanoemulsions made with 30 mM h-decanoate, in D_2O, in the ppp polarization scheme, and with d-hexadecane. This polarization combination accesses different elements of the $\Gamma^{(2)}$ tensor and thus can measure vibrational modes not present in the ssp spectra. For this system, this allows for the monitoring of an additional vibrational resonance, the CH_3 asymmetric stretch at 2962 cm^{-1}.[28,48] The spectra in Figure 5 were globally fit together. The spectra show an elevated background intensity, similar to the one shown in ssp spectra but slightly more pronounced due to the change in polarization. The inclusion of this background in the fits follows the same procedure as the ssp spectra, described in the Supporting Information. The modes increase in amplitude (Table S4) consistent with visual inspection of a rise in intensity for all modes indicating the fitting is accounting accurately for the probed resonance. The CH_3 asymmetric stretch increases in intensity as the pH environment goes from basic to acidic (green to red), following the trend observed previously in Figure 4. This indicates the surfactant tails are more conformationally ordered on the interface at the more acidic pH, giving rise to a strong response from this resonance. The ppp data coupled with ssp data indicate the surfactant layer on the nanoemulsion surface in the more acidic solution (red traces) is more conformationally ordered and thus could facilitate a more tightly packed monolayer. This type of monolayer indicates individual surfactants are positioned close enough to each other such that interactions between headgroups are likely. This implies the nanodroplet surface facilitates an environment that promotes the adsorption of the neutral, carboxylic acid surfactant. The nature of these interactions is further explored by probing the headgroup vibrational modes, as described below.

To allow distinction between the population of the charged and neutral form of the surfactant on the droplet surface, two additional spectral regions were investigated: the carboxylate stretch region (1300−1500 cm^{-1} region) and carbonyl stretch region (1600−1800 cm^{-1} region). Figure 6 shows carboxylate

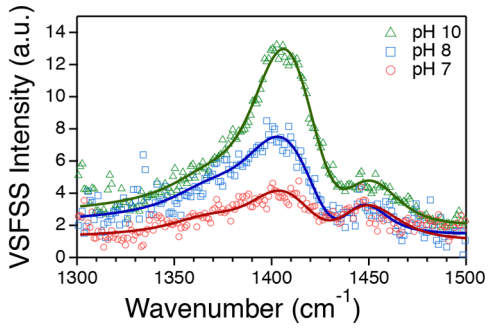

Figure 6. VSFSS in the carboxylate symmetric stretching region, in ssp polarization for 30 mM sodium decanoate (deuterated) stabilized nanoemulsions in H_2O at pH 7 (red circles), pH 8 (blue squares), and pH 10 (green triangles). Spectra were globally fit, with solid lines representing the fits to each spectrum.

VSFSS data in the ssp polarization combination for nanoemulsions stabilized with 30 mM d-decanoate, in H_2O, as a function of pH, and with d-hexadecane. The spectra were globally fit to three peaks assigned at 1437 ± 2, 1417 ± 3, and 1376 ± 6 cm^{-1}. All three peaks are assigned to the carboxylate symmetric stretch modes with different degrees of headgroup solvation.[8,18−21,23,59] This is consistent with previous measurements and assignments of multiple peaks of surface adsorbed carboxylate headgroups at the oil/water,[8,18,60] and air/water[19−21,23,59] interfaces. We attribute the 1376 and 1417 cm^{-1} peaks to headgroups with higher and lower degrees of solvation, respectively. Previous planar oil/water studies with CCl_4 as the organic phase show similar peaks and assignments at ∼1365 and ∼1405 cm^{-1}.[18] In the data from these previous planar studies, a weak peak in the range of 1440 cm^{-1} is

https://doi.org/10.1021/acs.jpcb.1c05508
J. Phys. Chem. B 2021, 125, 9629−9640

discernible in the ppp spectrum but was not analyzed. That we see the 1437 cm^{-1} peak more strongly in these nanoemulsions studies could be due to the difference in organic solvent or stronger dipole orientation on the interface. A shift of the carboxylate symmetric stretch to higher frequencies (1475 cm^{-1}) has been observed with sum frequency at the air/water interface for carboxylate surfactants in the presence of ions.[23,59] For planar oil/water sum frequency studies of carboxylic acid containing peptoid nanosheets, a peak at 1440 cm^{-1} is observed and assigned to the formation of contact ion pairs with NH_3^+ groups on the nanosheet.[60] In both these instances, the shift to higher frequencies is concluded to arise from a change in the solvation of the headgroup due to an ionic interaction with counterions. Thus, we conclude the 1437 cm^{-1} peak is indicative of a carboxylate headgroup with the lowest degree of solvation, which would result from a closer interaction of the sodium counterion and subsequent reduction in solvation.

The signal decreases for all peaks in the carboxylate region (Figure 6) as the conditions go from pH 10 where the bulk surfactant is fully deprotonated to pH 7 where the bulk surfactant is close to an equal mixture of the protonated and deprotonated forms. From ζ-potential measurements (Figure 3) we have shown that the pH does not greatly affect the adsorption of carboxylate surfactant. Thus, the loss of this VSFSS response due to pH must arise from something other than the loss of carboxylate surfactant population from the interface. A discussion on the possible effect of ionic strength is given in the Supporting Information. From the CH data, we know that as pH is lowered, there is increasing population of the carboxylic acid surfactant at the interface, likely accompanied by increased headgroup interactions between ionic and neutral headgroups. We therefore attribute this decrease in sum frequency response in Figure 6 to a change in orientation of the carboxylate headgroup as it forms acid−anion complexes with neighboring carboxylic acid surfactants. With such an interaction, it may be expected that a new spectral signature would appear for these complexes. There have been reports of a carbonyl vibrational mode at 1620 cm^{-1} for FTIR studies of ionomer films with carboxylate−carboxylic acid complexes.[61,62] However, previous sum frequency and IRRAS studies of carboxylic acid/carboxylate surfactants forming these complexes at the air/water interface and bulk FTIR studies of aqueous carboxylic acid surfactants have not observed such a spectral feature.[17,63,64] Therefore, it is not unexpected that we do not observe this vibrational signature in our studies (as evident in the carbonyl spectra below). We thus conclude that the loss in intensity for these peaks with pH is a result of acid−anion complex formation, leading to a change in the net orientation of the carboxylate headgroup.

Before analyzing the carbonyl vibrational signature of the C═O stretching mode in the 1600−1800 cm^{-1} region, a comment on the experimental difficulties is warranted. In our initial sum frequency scattering experiments for decanoate stabilized emulsions in this region (Figure S2), we found a significant background contribution present which obscures detection and analysis of this mode. Recent VSFSS studies in this spectral region by Schmüser et al.[39] have found a similar significant background, which they attribute to a nonlinear response from the CaF_2 window of VSFSS cuvettes. They confirmed this by use of a windowless VSFSS setup that exhibits no background response. In our case, to partially overcome this background, a well-established method of detiming the visible pulse from the IR pulse was employed.[65] This method allows for the selective detection of longer lasting vibrational modes over shorter-lived modes. Required in this setup is an etalon to shape the visible pulse to have a time asymmetric profile with a steep dropoff. This detiming method is often done in the CH stretching region to reduce contributions from H_2O[66] and in work on solid interfaces (i.e., gold) to reduce nonresonant contributions.[67] Figure 7 shows the carefully detimed (500−600 fs) carbonyl data for 30 mM h-decanoate as a function of pH and the surfactant h-AOT stabilized nanoemulsions (Figure 7, lower panel) as a function of concentration, in both D_2O, with ssp polarization, and h-hexadecane. The ester containing surfactant AOT was used as a reference to confirm the peaks present are arising from a carbonyl response. Discernible peaks are clearly present, showing that the carbonyl response can be observed. Although the background response is diminished, it is still present in the spectra in Figure 7, making this detiming method more limited in its applicability but still useful for experimental geometries, such as used here, in which it is difficult to produce a windowless setup.

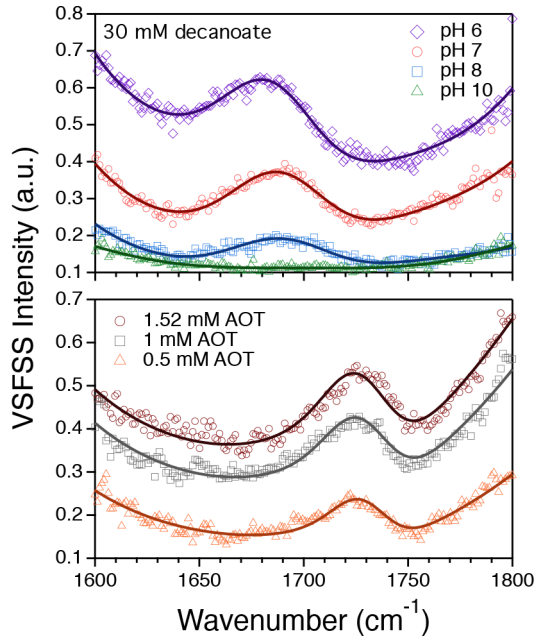

Figure 7. VSFSS spectra (ssp polarization) in the carbonyl stretching region, in ssp polarization for 30 mM decanoate stabilized nanoemulsions with h-hexadecane, in D_2O (top panel) at pH 6 (purple diamonds), 7 (red circles), 8 (blue squares), and 10 (green triangles). Nanoemulsions stabilized with the ester containing surfactant AOT (bottom panel) as a function of concentration was used as a reference to confirm the peaks present are arising from a carbonyl response. Spectra are not offset from each other; the elevated background arises from a nonlinear response from the CaF_2 window of the VSFSS cuvette, which is reduced by detiming the visible pulse from the IR pulse. Spectra were globally fit, with solid lines representing fits to each spectrum (see the Supporting Information for how the background spectral shape was determined).

When fitting this spectral region, the spectral shape of the background response needs to be taken into account to derive any meaningful analysis. The method for determining the background spectral shape is given in detail in the Supporting Information. Briefly, the broad initial response was fit with one peak at low wavenumbers to capture a broad, decaying spectral

https://doi.org/10.1021/acs.jpcb.1c05508
J. Phys. Chem. B 2021, 125, 9629−9640

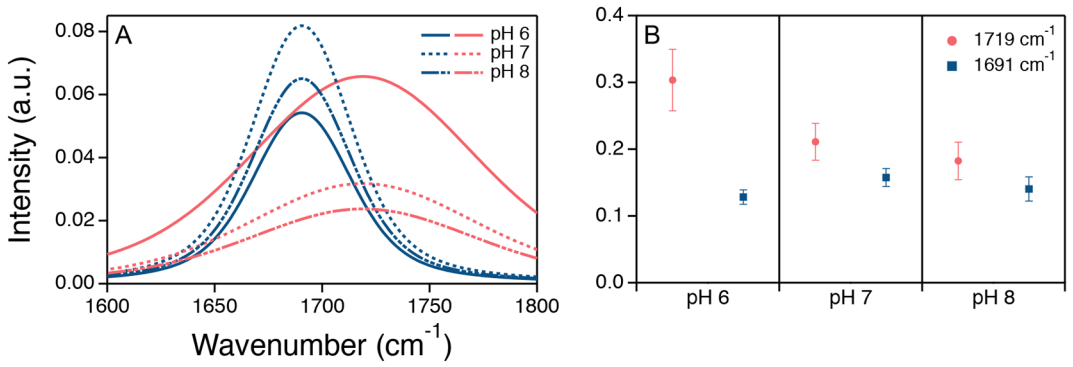

Figure 8. (A) Individual peaks from the fits in Figure 7 for 30 mM decanoate at pH 6 (solid lines), 7 (dashed lines), and 8 (dashed and dotted lines). Pink traces are the 1719 cm^{-1} peak, and blue traces are the 1691 cm^{-1} peak. (B) Amplitudes from the fits in Figure 7; pink circles are the 1719 cm^{-1} peak, and blue squares are the 1691 cm^{-1} peak.

shape. Next, the pH 10 spectrum was fit by using the low wavenumber peak and a peak at higher wavenumbers to capture the U-shaped background spectral response. The pH 10 spectrum has no carbonyl response; therefore, it only contains the background contributions. The carbonyl resonances in Figure 7 were then globally fit, with every parameter accounting for the background spectral shape held constant except the amplitudes. From the fits, the carbonyl for the AOT nanoemulsion system is found to be at 1731 ± 0.3 cm^{-1}, which agrees with other bulk (1735 cm^{-1})[68] reports of this carbonyl. Additionally, the amplitude of the resonance increases with increasing concentration, indicating that the fitting is accounting as accurately as possible for both peak positions and amplitudes of the probed resonance. It should be noted that impairment of the fit analysis in the carbonyl region due to the overlapping background modes is still a possibility.

For the decanoate nanoemulsion system, no carbonyl response is seen in Figure 7 (top panel) at pH 10 (green triangles), whereas a response is present for pH 8 (blue squares), 7 (red circles), and 6 (purple diamonds). While the background response significantly interferes with the probed resonance, from our analysis this carbonyl is most accurately fit with two carbonyl peaks at 1691 ± 0.6 and 1719 ± 5.2 cm^{-1} (Figure 7, upper panel). Figure 8A shows the spectral contributions from the individual peaks derived from spectral fitting. Figure 8B shows the amplitudes from the fits in the carbonyl spectra. The spectral characteristics of these peaks are distinctly different in frequency, breadth, and pH dependence, reflective of at least two very different headgroup surface environments. As shown in Figure 8, the broad peak at 1719 cm^{-1} (pink traces) shows a sharp reduction in intensity with increasing pH. The sharper peak at 1691 cm^{-1} (blue traces) stays nearly constant within experimental uncertainty, with a slightly favored signal at pH 7. The broadness of the 1719 cm^{-1} peak (pink traces) illustrates that this carbonyl has a relatively large distribution of headgroup environments. The 1691 cm^{-1} peak (blue traces) is narrower, reflective of a more highly oriented and/or distinct solvation environment at the interface relative to the higher frequency peak.

We attribute the 1691 cm^{-1} peak to the formation of acid−acid dimers. These dimers consist of two carboxylic acid units that are hydrogen bonded to each other, such that the carbonyl of one is interacting with the OH of the other. Although increasing water solvation is typically associated with red-shifted carbonyl modes,[69,70] we base our assignment on FTIR studies of bulk carboxylic acid surfactant mixtures where a similar peak at 1690 cm^{-1} is attributed to such dimers.[71−73] Additionally, computational investigations of carboxylic acid self-assembled monolayers have shown such interactions to occur.[74] These acid−acid dimers form between two protonated, carboxylic acid headgroups. We believe that in order for this to happen the protonated headgroups have to be clustered in such a way that promotes these interactions. We have shown the carboxylate species present on the interface recruits protonated, carboxylic acid species to populate the interface as the pH is lowered, which could cause these surfactants to cluster, giving rise to this acid−acid interaction. The constancy in the 1691 cm^{-1} response fit to here is consistent with a limited number of carboxylate surface species with which these clusters can form. The increase in proximity of the headgroups in these surfactant clusters allows the carbonyls of the carboxylic acid groups to interact in such a way that they can hydrogen bond with each other giving rise to the peak at 1691 cm^{-1}.

The 1719 cm^{-1} peak is assigned as a lone carboxylic acid unit that is only weakly interacting with neighboring surfactants. This assignment is based on previous sum frequency studies of carboxylic acid surfactants[18] and sum frequency studies of the polymer poly(acrylic acid) at the planar oil/water interface.[75] The previous studies of the carboxylic acid surfactants show the carbonyl response having a very weak signal only at pH 2 and at a frequency of 1740 cm^{-1}. Additionally, no discernible carbonyl response is observed above that pH.[18] A strong and relatively sharp carbonyl response at 1730 cm^{-1} is observed for the carboxylic acid containing polymer, poly(acrylic acid) , at the planar oil/water interface at pH 2−4.5.[75] In that case, the polymer carboxylic acid acts as a lone and highly oriented carbonyl, experiencing no significant interactions with neighboring polymer units. The shift to lower wavenumbers and the breadth of the peak in this study compared to the planar studies, however, are evident of various weak interactions with nearby carboxylic acid and carboxylate groups that would recruit the neutral surfactant to the interface. As the pH is lowered, the increase in intensity of the carbonyl response in Figure 7 is reflective of the increase in carboxylic acid surfactant bulk and subsequent surface population and net orientation. This indicates increased adsorption of the lone carboxylic acid that is not significantly participating in acid−anion or acid−acid complexes.

The overall results show distinct differences to what is observed at the planar oil/water interface. The very different spectral characteristics of this carbonyl mode seen in our

https://doi.org/10.1021/acs.jpcb.1c05508
J. Phys. Chem. B 2021, 125, 9629−9640

studies relative to the analogous surfactant at the planar oil/water surface are evidence that the carboxylic acid headgroup environment on the nanodroplet surface is much more complex. Sum frequency experiments at the planar oil/water interface have shown that there is preferential adsorption of the charged carboxylate over the neutral carboxylic acid species at all pHs where carboxylate is present.[18] Computational studies of the protonated carboxylic acid surfactant on its own at the oil/water planar interface have shown that although the protonated surfactant is present, it lacks interfacial conformational ordering, leading to minimal change in interfacial tension.[25] It is interesting, then, that we have documented such increased adsorption and interfacial orientation of the carboxylic acid surfactant and its headgroup at lower pHs on the nanodroplet surface. Additionally, the enhancement of surface population at the nanodroplet surface is not equal for both forms of the surfactant. Rather, the neutral carboxylic acid surfactant significantly contributes to the nanodroplet monolayer complexity with pH, while the charged carboxylate surfactant remains relatively stagnant but still acts as the primary source of stability for the droplets.

Figure 9 depicts the various forms of the surfactant adsorption occurring at the nanoemulsion interface. The fully

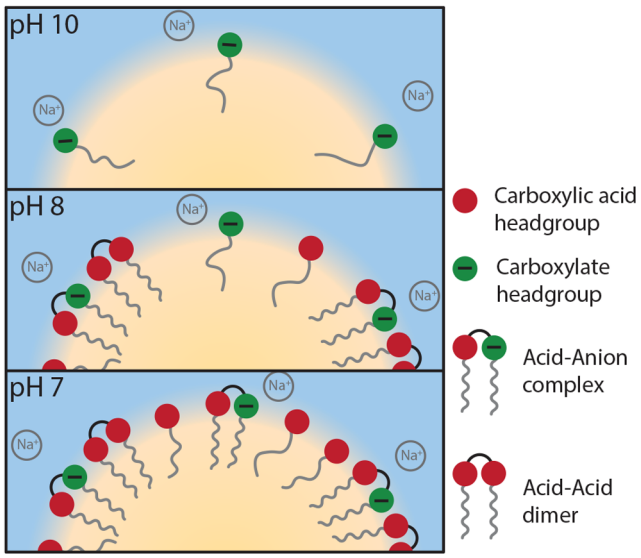

Figure 9. Cartoon depiction of the nanoemulsion surface. Three pH conditions are shown: pH 10 (top panel), pH 8 (middle panel), and pH 7 (bottom panel). The interface increases in complexity as the pH is lowered. The acid−acid dimer corresponds to the carbonyl frequency of 1691 cm^{-1}. The lone carboxylic acid headgroup (red circle) corresponds to the carbonyl peak of 1719 cm^{-1}. The lone carboxylate headgroup (green circle) corresponds to the carboxylate stretch in the 1300−1500 cm^{-1} region. In all three panels the amount of carboxylate headgroup (green) remains constant, and the higher ordering of the surfactant alkyl tails with a lower pH, as shown, is due to an increase in chain−chain hydrophobic interactions.

deprotonated surfactant mixture (pH 10, top section) has a dilute monolayer of carboxylate surfactant at the interface, and the amount of carboxylate remains constant across all three pH conditions (green headgroups). As the mixture reaches a combination of charged and uncharged forms with decreasing pH, complex interactions occur between the two headgroups, leading to clusters of hydrogen-bonded carboxylic acid units. At pH 8 (middle section) and pH 7 (lower section) the carboxylic acid surfactant forms acid−anion pairs consisting of complexation with a carboxylate group and acid−acid dimers consisting of two hydrogen-bonded carboxylic acid units. This interfacial structure is not, however, the simple picture of switching on/off interfacial activity with changing percent protonation. Rather, this shows with a mixture of protonated and deprotonated surfactant hydrogen-bonding interactions occur between the headgroups causing an increase in adsorption and complexity on the emulsion surface, while still able to stabilize the droplet.

SUMMARY AND CONCLUSION

Understanding the molecular properties of carboxylic acid surfactant adsorption is important as it can help to illuminate the key roles this functional group plays in systems such as biological organisms, industrial surfactant products, and the environment. In this paper, we have used a combination of ζ-potential, dynamic light scattering, and vibrational sum frequency scattering spectroscopy to demonstrate the unique interfacial behavior of carboxylic acid containing surfactants on nanoemulsion surfaces as a function of pH. The nanoemulsions are found to be stable in the range of pH 5.5−10, in which the bulk solution goes progressively from majority protonated species to all deprotonated charged species, based on acid−base equilibrium. The composition of the surface, however, does not mirror this bulk equilibrium. Rather, when the bulk mixture contains only carboxylic acid surfactant (pH 4 and below), the nanoemulsions quickly destabilize and separate into oil and water layers. The stable nanoemulsions between pH 5.5 and 10 exhibit a constant negative ζ-potential value, reflective of a surface population of charged carboxylate species that does not vary with pH. This is in contrast to the large increase in bulk carboxylate surfactant with rising pH. Thus, it is concluded the carboxylate surfactant reaches its maximum surface concentration at a pH as low as 5.5, when there is little carboxylate in the bulk. This conclusion indicates the amount of carboxylate at the interface is small compared to that of the bulk.

VSFSS in the CH stretching region shows remarkably different behavior for the adsorption of the protonated surfactant in the stable nanoemulsion region. The constancy in the carboxylate surface concentration as the pH is lowered to 5.5 contrasts to a significant growth in surface population of the carboxylic acid surfactant. The monolayer adopts a more conformationally ordered structure, confirming that the density of surfactants at the surface is in fact increasing. The spectroscopy of the headgroup region provides evidence for clustering and bonding interactions between neighboring charged and uncharged surfactants. Spectra in the carboxylate stretching region show the formation of acid−anion complexes in which a carboxylic acid and a carboxylate share a proton, often seen at the air/water interface. The carbonyl spectra show a shift in the frequency position to what is found in planar oil/water studies, representing clusters of hydrogen-bonded carboxylic acid headgroups at the nanodroplet surface. These carboxylic acid clusters are recruited and stabilized at the interface through the interactions with the carboxylate headgroup.

This increase in carboxylic acid surfactant adsorption as the pH is lowered is interesting for a couple reasons. First, the neutral, carboxylic acid on its own is insufficient at stabilizing the droplet, and second, planar studies of the oil/water interface show that the neutral carboxylic acid surfactant does

https://doi.org/10.1021/acs.jpcb.1c05508
J. Phys. Chem. B 2021, 125, 9629−9640

not exhibit significant adsorption at any pH. This implies that the interactions we have observed in this study are unique to the droplet surface. To form a stable droplet, it is necessary to introduce surfactants, in this case a charged alkyl surfactant, to prevent any coalescence into the thermodynamically favored planar, phase-separated surface. The differences between these two interfaces affect how the carboxylate (charged) and carboxylic acid (neutral) surfactants adsorb. The carboxylate surfactants experience charge−charge repulsion between each other, resulting in an interfacial concentration necessary to stabilize the droplet that is small compared to the bulk concentration and is invariant with pH, while the neutral species experiences no repulsive forces and so increasingly adsorbs to the surface as pH is lowered. This increase in adsorption contributes to a more densely packed monolayer through the formation of hydrogen-bonded clusters of the two forms of surfactant. Again, the actual interfacial charge is the same in this region, and the complexity is delivered through the adsorption of the neutral carboxylic acid surfactant. Thus, while charge is the main stabilizing force for these droplets, the interfacial structure of the monolayer is greatly affected by the neutral, uncharged surfactant. The droplet surface is therefore different than the planar interface in that it promotes dynamic interactions between the surfactant headgroups affecting their adsorption behavior.

The results presented here show that carboxylic acid and carboxylate functional groups interact strongly with each other to form complex monolayers on droplet surfaces. That the two forms of the headgroups have a dynamic adsorption behavior with pH at the nanodroplet surface is important for many applications in industrial, environmental, and biological systems. The two surfactants cannot be thought of independently in their adsorption or surface chemistry on hydrophobic/aqueous droplet surfaces. In addition, this study shows the importance of investigating the molecular details of nanodroplet systems to understand the factors contributing to their stabilization.

■ ASSOCIATED CONTENT

Supporting Information

The Supporting Information is available free of charge at https://pubs.acs.org/doi/10.1021/acs.jpcb.1c05508.

Chemical structures of carboxylate and AOT surfactants, stability studies, percent protonation based on acid−base equilibrium derivation, ζ-potential of sodium octanoate and dodecanoate stabilized nanoemulsions, d^+/r^+ ratio analysis for CH stretching region, comment on low-wavenumber background in CH data, comment on the effect of ionic strength in the carboxylate spectra, carbonyl background spectral shape determination, and fit parameters for all spectra (PDF)

■ AUTHOR INFORMATION

Corresponding Author

Geraldine L. Richmond − *Department of Chemistry and Biochemistry, University of Oregon, Eugene, Oregon 97405, United States;* orcid.org/0000-0003-0876-5262; Email: richmond@uoregon.edu

Authors

Marc J. Foster − *Department of Chemistry and Biochemistry, University of Oregon, Eugene, Oregon 97405, United States*

Andrew P. Carpenter − *Department of Chemistry and Biochemistry, University of Oregon, Eugene, Oregon 97405, United States;* orcid.org/0000-0003-1020-1706

Complete contact information is available at: https://pubs.acs.org/10.1021/acs.jpcb.1c05508

Notes

The authors declare no competing financial interest.

■ ACKNOWLEDGMENTS

The authors thank Emma Tran and Dr. Rebecca Altman for helpful discussions on both the technical data collection and analysis of the results in this study. This material is based upon work supported by the National Science Foundation, Award CHE-2000356, and the National Science Foundation Graduate Research Fellowship for M. J. Foster under Grant DGE-1842486.

■ REFERENCES

(1) Kujawinski, E. B.; Reddy, C. M.; Rodgers, R. P.; Thrash, J. C.; Valentine, D. L.; White, H. K. The first decade of scientific insights from the deepwater horizon oil release. *Nature Reviews Earth & Environment* **2020**, *1* (5), 237−250.

(2) Attia, M. F.; Dieng, S. M.; Collot, M.; Klymchenko, A. S.; Bouillot, C.; Serra, C. A.; Schmutz, M.; Er-Rafik, M.; Vandamme, T. F.; Anton, N. Functionalizing nanoemulsions with carboxylates: Impact on the biodistribution and pharmacokinetics in mice. *Macromol. Biosci.* **2017**, *17* (7), 1600471.

(3) Cheng, L.-C.; Hashemnejad, S. M.; Zarket, B.; Muthukrishnan, S.; Doyle, P. S. Thermally and ph-responsive gelation of nanoemulsions stabilized by weak acid surfactants. *J. Colloid Interface Sci.* **2020**, *563*, 229−240.

(4) Guerra, F. D.; Attia, M. F.; Whitehead, D. C.; Alexis, F. Nanotechnology for environmental remediation: Materials and applications. *Molecules* **2018**, *23* (7), 1760.

(5) Lee, R.; Hagen, W; Kattner, G Lipid storage in marine zooplankton. *Mar. Ecol.: Prog. Ser.* **2006**, *307*, 273−306.

(6) Johansson, I.; Svensson, M. Surfactants based on fatty acids and other natural hydrophobes. *Curr. Opin. Colloid Interface Sci.* **2001**, *6* (2), 178−188.

(7) Liu, Y.; Jessop, P. G.; Cunningham, M.; Eckert, C. A.; Liotta, C. L. Switchable surfactants. *Science* **2006**, *313* (5789), 958−960.

(8) Robertson, E. J.; Beaman, D. K.; Richmond, G. L. Designated drivers: The differing roles of divalent metal ions in surfactant adsorption at the oil-water interface. *Langmuir* **2013**, *29* (50), 15511−15520.

(9) Keleşoğlu, S.; Meakin, P.; Sjöblom, J. Effect of aqueous phase ph on the dynamic interfacial tension of acidic crude oils and myristic acid in dodecane. *J. Dispersion Sci. Technol.* **2011**, *32* (11), 1682−1691.

(10) Serri, N.; Kamarudin, A.; Rahaman, A. Preliminary studies for production of fatty acids from hydrolysis of cooking palm oil using c. Rugosa lipase. *J. Phys. Sci.* **2008**, *19* (1), 79−88.

(11) Xu, W.; Gu, H.; Zhu, X.; Zhong, Y.; Jiang, L.; Xu, M.; Song, A.; Hao, J. Co2-controllable foaming and emulsification properties of the stearic acid soap systems. *Langmuir* **2015**, *31* (21), 5758−5766.

(12) Agarwal, A.; Liu, Y. Remediation technologies for oil-contaminated sediments. *Mar. Pollut. Bull.* **2015**, *101* (2), 483−490.

(13) Lu, Y.; Sun, D.; Ralston, J.; Liu, Q.; Xu, Z. Co2-responsive surfactants with tunable switching ph. *J. Colloid Interface Sci.* **2019**, *557*, 185−195.

(14) Alshamrani, A. K.; Vanderveen, J. R.; Jessop, P. G. A guide to the selection of switchable functional groups for co2-switchable compounds. *Phys. Chem. Chem. Phys.* **2016**, *18* (28), 19276−19288.

(15) Ceschia, E.; Harjani, J. R.; Liang, C.; Ghoshouni, Z.; Andrea, T.; Brown, R. S.; Jessop, P. G. Switchable anionic surfactants for the

remediation of oil-contaminated sand by soil washing. *RSC Adv.* **2014**, *4* (9), 4638−4645.
(16) Xu, P.; Wang, Z.; Xu, Z.; Hao, J.; Sun, D. Highly effective emulsification/demulsification with a co2-switchable superamphiphile. *J. Colloid Interface Sci.* **2016**, *480*, 198−204.
(17) Andino, R. S.; Liu, J.; Miller, C. M.; Chen, X.; Devlin, S. W.; Hong, M. K.; Rajagopal, R.; Erramilli, S.; Ziegler, L. D. Anomalous ph-dependent enhancement of p-methyl benzoic acid sum-frequency intensities: Cooperative surface adsorption effects. *J. Phys. Chem. A* **2020**, *124* (16), 3064−3076.
(18) Beaman, D. K.; Robertson, E. J.; Richmond, G. L. From head to tail: Structure, solvation, and hydrogen bonding of carboxylate surfactants at the organic-water interface. *J. Phys. Chem. C* **2011**, *115* (25), 12508−12516.
(19) Tyrode, E.; Corkery, R. Charging of carboxylic acid monolayers with monovalent ions at low ionic strengths: Molecular insight revealed by vibrational sum frequency spectroscopy. *J. Phys. Chem. C* **2018**, *122* (50), 28775−28786.
(20) Sthoer, A.; Tyrode, E. Interactions of na+ cations with a highly charged fatty acid langmuir monolayer: Molecular description of the phase transition. *J. Phys. Chem. C* **2019**, *123* (37), 23037−23048.
(21) Sthoer, A.; Hladílková, J.; Lund, M.; Tyrode, E. Molecular insight into carboxylic acid-alkali metal cations interactions: Reversed affinities and ion-pair formation revealed by non-linear optics and simulations. *Phys. Chem. Chem. Phys.* **2019**, *21* (21), 11329−11344.
(22) Wellen, B. A.; Lach, E. A.; Allen, H. C. Surface pka of octanoic, nonanoic, and decanoic fatty acids at the air-water interface: Applications to atmospheric aerosol chemistry. *Phys. Chem. Chem. Phys.* **2017**, *19* (39), 26551−26558.
(23) Tang, C. Y.; Huang, Z.; Allen, H. C. Binding of mg2+ and ca2+ to palmitic acid and deprotonation of the cooh headgroup studied by vibrational sum frequency generation spectroscopy. *J. Phys. Chem. B* **2010**, *114* (51), 17068−17076.
(24) Konek, C. T.; Musorrafiti, M. J.; Al-Abadleh, H. A.; Bertin, P. A.; Nguyen, S. T.; Geiger, F. M. Interfacial acidities, charge densities, potentials, and energies of carboxylic acid-functionalized silica/water interfaces determined by second harmonic generation. *J. Am. Chem. Soc.* **2004**, *126* (38), 11754−11755.
(25) Holte, L. K.; Kuran, B. A.; Richmond, G. L.; Johnson, K. E. Computational modeling of lauric acid at the organic-water interface. *J. Phys. Chem. C* **2014**, *118* (19), 10024−10032.
(26) McClements, D. J. Nanoemulsions versus microemulsions: Terminology, differences, and similarities. *Soft Matter* **2012**, *8* (6), 1719−1729.
(27) Gupta, A.; Eral, H. B.; Hatton, T. A.; Doyle, P. S. Nanoemulsions: Formation, properties and applications. *Soft Matter* **2016**, *12* (11), 2826−2841.
(28) Chen, Y.; Jena, K. C.; Roke, S. From hydrophobic to hydrophilic: The structure and density of the hexadecane droplet/alkanol/water interface. *J. Phys. Chem. C* **2015**, *119* (31), 17725−17734.
(29) de Aguiar, H. B.; de Beer, A. G. F.; Strader, M. L.; Roke, S. The interfacial tension of nanoscopic oil droplets in water is hardly affected by sds surfactant. *J. Am. Chem. Soc.* **2010**, *132* (7), 2122−2123.
(30) de Aguiar, H. B.; Strader, M. L.; de Beer, A. G. F.; Roke, S. Surface structure of sodium dodecyl sulfate surfactant and oil at the oil-in-water droplet liquid/liquid interface: A manifestation of a nonequilibrium surface state. *J. Phys. Chem. B* **2011**, *115* (12), 2970−2978.
(31) Roke, S.; Roeterdink, W. G.; Wijnhoven, J. E. G. J.; Petukhov, A. V.; Kleyn, A. W.; Bonn, M. Vibrational sum frequency scattering from a submicron suspension. *Phys. Rev. Lett.* **2003**, *91* (25), 258302.
(32) Smolentsev, N.; Smit, W. J.; Bakker, H. J.; Roke, S. The interfacial structure of water droplets in a hydrophobic liquid. *Nat. Commun.* **2017**, *8* (1), 15548.
(33) Zdrali, E.; Chen, Y.; Okur, H. I.; Wilkins, D. M.; Roke, S. The molecular mechanism of nanodroplet stability. *ACS Nano* **2017**, *11* (12), 12111−12120.
(34) Zdrali, E.; Etienne, G.; Smolentsev, N.; Amstad, E.; Roke, S. The interfacial structure of nano- and micron-sized oil and water droplets stabilized with sds and span80. *J. Chem. Phys.* **2019**, *150* (20), 204704.
(35) Tran, E.; Carpenter, A. P.; Richmond, G. L. Probing the molecular structure of coadsorbed polyethylenimine and charged surfactants at the nanoemulsion droplet surface. *Langmuir* **2020**, *36* (31), 9081−9089.
(36) Hensel, J. K.; Carpenter, A. P.; Ciszewski, R. K.; Schabes, B. K.; Kittredge, C. T.; Moore, F. G.; Richmond, G. L. Molecular characterization of water and surfactant aot at nanoemulsion surfaces. *Proc. Natl. Acad. Sci. U. S. A.* **2017**, *114* (51), 13351−13356.
(37) Johansson, P. K.; Koelsch, P. Vibrational sum-frequency scattering for detailed studies of collagen fibers in aqueous environments. *J. Am. Chem. Soc.* **2014**, *136* (39), 13598−13601.
(38) Johansson, P. K.; Castner, D. G. Vibrational sum-frequency scattering as a sensitive approach to detect structural changes in collagen fibers treated with surfactants. *Langmuir* **2019**, *35* (24), 7848−7857.
(39) Schmüser, L.; Golbek, T. W.; Weidner, T. Windowless detection geometry for sum frequency scattering spectroscopy in the c-d and amide i regions. *Biointerphases* **2021**, *16* (1), 011201.
(40) Krężel, A.; Bal, W. A formula for correlating pka values determined in d2o and h2o. *J. Inorg. Biochem.* **2004**, *98* (1), 161−166.
(41) González-Pérez, A.; Ruso, J. M.; Prieto, G.; Sarmiento, F. Apparent molar quantities of sodium octanoate in aqueous solutions. *Colloid Polym. Sci.* **2004**, *282* (10), 1133−1139.
(42) Mukerjee, P.; Mysels, K. J. Critical micelle concentrations of aqueous surfactant systems; National Standard reference data system, 1971.
(43) Ohno, P. E.; Wang, H.-f.; Geiger, F. M. Second-order spectral lineshapes from charged interfaces. *Nat. Commun.* **2017**, *8* (1), 1032.
(44) Guyot-Sionnest, P.; Hunt, J. H.; Shen, Y. R. Sum-frequency vibrational spectroscopy of a langmuir film: Study of molecular orientation of a two-dimensional system. *Phys. Rev. Lett.* **1987**, *59* (14), 1597−1600.
(45) Lambert, A. G.; Davies, P. B.; Neivandt, D. J. Implementing the theory of sum frequency generation vibrational spectroscopy: A tutorial review. *Appl. Spectrosc. Rev.* **2005**, *40* (2), 103−145.
(46) Hunt, J.; Guyot-Sionnest, P.; Shen, Y. Observation of ch stretch vibrations of monolayers of molecules optical sum-frequency generation. *Chem. Phys. Lett.* **1987**, *133* (3), 189−192.
(47) Zhu, X.; Suhr, H.; Shen, Y. Surface vibrational spectroscopy by infrared-visible sum frequency generation. *Phys. Rev. B: Condens. Matter Mater. Phys.* **1987**, *35* (6), 3047.
(48) de Beer, A. G. F.; Roke, S. Sum frequency generation scattering from the interface of an isotropic particle: Geometrical and chiral effects. *Phys. Rev. B: Condens. Matter Mater. Phys.* **2007**, *75* (24), 245438.
(49) Blower, P. G.; Shamay, E.; Kringle, L.; Ota, S. T.; Richmond, G. L. Surface behavior of malonic acid adsorption at the air/water interface. *J. Phys. Chem. A* **2013**, *117* (12), 2529−2542.
(50) Bain, C. D.; Davies, P. B.; Ong, T. H.; Ward, R. N.; Brown, M. A. The structure of interfaces probed by sum-frequency spectroscopy. *Surf. Interface Anal.* **1991**, *17* (7), 529−530.
(51) Kanicky, J. R.; Poniatowski, A. F.; Mehta, N. R.; Shah, D. O. Cooperativity among molecules at interfaces in relation to various technological processes: Effect of chain length on the pka of fatty acid salt solutions. *Langmuir* **2000**, *16* (1), 172−177.
(52) Bain, C. D.; Whitesides, G. M. A study by contact angle of the acid-base behavior of monolayers containing. Omega.-mercaptocarboxylic acids adsorbed on gold: An example of reactive spreading. *Langmuir* **1989**, *5* (6), 1370−1378.
(53) Wang, D.; Nap, R. J.; Lagzi, I. N.; Kowalczyk, B.; Han, S.; Grzybowski, B. A.; Szleifer, I. How and why nanoparticle's curvature regulates the apparent pkaof the coating ligands. *J. Am. Chem. Soc.* **2011**, *133* (7), 2192−2197.

https://doi.org/10.1021/acs.jpcb.1c05508
J. Phys. Chem. B 2021, 125, 9629−9640

(54) Kanicky, J. R.; Shah, D. O. Effect of premicellar aggregation on the pka of fatty acid soap solutions. *Langmuir* **2003**, *19* (6), 2034−2038.
(55) Rajagopal, R.; Hong, M. K.; Ziegler, L. D.; Erramilli, S.; Narayan, O. Conjugate acid-base interaction driven phase transition at a 2d air-water interface. *J. Phys. Chem. B* **2021**, *125*, 6330.
(56) Carpenter, A. P.; Foster, M. J.; Jones, K. K.; Richmond, G. L. Effects of salt-induced charge screening on aot adsorption to the planar and nanoemulsion oil-water interfaces. *Langmuir* **2021**, *37*, 8658.
(57) Conboy, J. C.; Messmer, M. C.; Richmond, G. L. Investigation of surfactant conformation and order at the liquid-liquid interface by total internal reflection sum-frequency vibrational spectroscopy. *J. Phys. Chem.* **1996**, *100* (18), 7617−7622.
(58) Scheu, R.; Chen, Y.; Subinya, M.; Roke, S. Stern layer formation induced by hydrophobic interactions: A molecular level study. *J. Am. Chem. Soc.* **2013**, *135* (51), 19330−19335.
(59) Tang, C. Y.; Allen, H. C. Ionic binding of na+ versus k+ to the carboxylic acid headgroup of palmitic acid monolayers studied by vibrational sum frequency generation spectroscopy. *J. Phys. Chem. A* **2009**, *113* (26), 7383−7393.
(60) Robertson, E. J.; Olivier, G. K.; Qian, M.; Proulx, C.; Zuckermann, R. N.; Richmond, G. L. Assembly and molecular order of two-dimensional peptoid nanosheets through the oil-water interface. *Proc. Natl. Acad. Sci. U. S. A.* **2014**, *111*, 201414843.
(61) Coleman, M. M.; Lee, J. Y.; Painter, P. C. Acid salts and the structure of ionomers. *Macromolecules* **1990**, *23* (8), 2339−2345.
(62) Haines, T. H. Anionic lipid headgroups as a proton-conducting pathway along the surface of membranes: A hypothesis. *Proc. Natl. Acad. Sci. U. S. A.* **1983**, *80* (1), 160−164.
(63) Wen, X.; Lauterbach, J.; Franses, E. I. Surface densities of adsorbed layers of aqueous sodium myristate inferred from surface tension and infrared reflection absorption spectroscopy. *Langmuir* **2000**, *16* (17), 6987−6994.
(64) Xu, W.; Song, A.; Dong, S.; Chen, J.; Hao, J. A systematic investigation and insight into the formation mechanism of bilayers of fatty acid/soap mixtures in aqueous solutions. *Langmuir* **2013**, *29* (40), 12380−12388.
(65) Khan, M. R.; Singh, H.; Sharma, S.; Asetre Cimatu, K. L. Direct observation of adsorption morphologies of cationic surfactants at the gold metal-liquid interface. *J. Phys. Chem. Lett.* **2020**, *11* (22), 9901−9906.
(66) Schulze-Zachau, F.; Bachmann, S.; Braunschweig, B. Effects of ca2+ ion condensation on the molecular structure of polystyrene sulfonate at air-water interfaces. *Langmuir* **2018**, *34* (39), 11714−11722.
(67) Lagutchev, A.; Hambir, S. A.; Dlott, D. D. Nonresonant background suppression in broadband vibrational sum-frequency generation spectroscopy. *J. Phys. Chem. C* **2007**, *111* (37), 13645−13647.
(68) Li, Q.; Weng, S.; Wu, J.; Zhou, N. Comparative study on structure of solubilized water in reversed micelles. 1. Ft-ir spectroscopic evidence of water/aot/n-heptane and water/nadehp/n-heptane systems. *J. Phys. Chem. B* **1998**, *102* (17), 3168−3174.
(69) Fried, S. D.; Bagchi, S.; Boxer, S. G. Measuring electrostatic fields in both hydrogen-bonding and non-hydrogen-bonding environments using carbonyl vibrational probes. *J. Am. Chem. Soc.* **2013**, *135* (30), 11181−11192.
(70) Choi, J.-H.; Cho, M. Vibrational solvatochromism and electrochromism of infrared probe molecules containing c≡o, c≡n, c = o, or c-f vibrational chromophore. *J. Chem. Phys.* **2011**, *134* (15), 154513.
(71) Lynch, M. L.; Pan, Y.; Laughlin, R. G. Spectroscopic and thermal characterization of 1:2 sodium soap/fatty acid acid-soap crystals. *J. Phys. Chem.* **1996**, *100* (1), 357−361.
(72) Doan, V.; Köppe, R.; Kasai, P. H. Dimerization of carboxylic acids and salts: An ir study in perfluoropolyether media. *J. Am. Chem. Soc.* **1997**, *119* (41), 9810−9815.
(73) Gershevitz, O.; Sukenik, C. N. In situ ftir-atr analysis and titration of carboxylic acid-terminated sams. *J. Am. Chem. Soc.* **2004**, *126* (2), 482−483.
(74) Winter, N.; Vieceli, J.; Benjamin, I. Hydrogen-bond structure and dynamics at the interface between water and carboxylic acid-functionalized self-assembled monolayers. *J. Phys. Chem. B* **2008**, *112* (2), 227−231.
(75) Robertson, E. J.; Richmond, G. L. Chunks of charge: Effects at play in the assembly of macromolecules at fluid surfaces. *Langmuir* **2013**, *29* (35), 10980−10989.

https://doi.org/10.1021/acs.jpcb.1c05508
J. Phys. Chem. B 2021, 125, 9629−9640